CHEMICAL ENGINEERING TRANSACTIONS
VOL. 82, 2020
A publication of AIDIC
The Italian Association of Chemical Engineering
Online at www.cetjournal.it
Guest Editors: Bruno Fabiano, Valerio Cozzani, Genserik Reniers

ISBN 978-88-95608-80-8; **ISSN** 2283-9216
DOI: 10.3303/CET2082063

LNG Tanks Exposed to Distant Pool Fires: a CFD Study

Tommaso Iannaccone[a], Giordano Emrys Scarponi[a], Gabriele Landucci[b], Valerio Cozzani[a]*

[a] LISES - Dipartimento di Ingegneria Civile, Chimica, Ambientale e dei Materiali, Alma Mater Studiorum - Università di Bologna, via Terracini n.28, 40131 Bologna, Italy.
[b] Dipartimento di Ingegneria Civile e Industriale, Università di Pisa, Largo Lucio Lazzarino 2, 56126 Pisa, Italy.
valerio.cozzani@unibo.it

Liquefied natural gas (LNG) is a viable, environmental-friendly alternative marine fuel. Several LNG-fueled vessels are already operating, and the LNG market is expected to grow further in the next years. A capillary marine LNG infrastructure network is developing to strengthen the fuel supply chain, which includes small-scale LNG storage and bunkering installations. However, safety remains a crucial aspect for the expansion of sustainable and reliable LNG technologies due to flammability hazards of natural gas. Storage tanks are vulnerable units from a safety point of view: external fires might affect LNG tanks leading to their catastrophic failure with a possibility of accident escalation. The present contribution aims at the evaluation of thermal response of storage tanks exposed to high levels of thermal radiation from distant sources, such as a pool fires generated after the ignition of LNG spills. A two-dimension computational fluid dynamic (CFD) approach is applied to predict tank pressurization rate and temperature distribution for a set of case studies. The results obtained give insight about the dynamic response of pressurized cryogenic vessels involved in process accidents, providing a useful contribution to emergency response planning as well as identifying important safety aspects regarding LNG storage and distribution chain.

1. Introduction

The International community is committed to achieve a reduction in pollutant emissions by introducing stringent environmental regulations, such as the International Maritime Organization (IMO) sulfur cap, which limits the sulfur content in maritime fuels. As a consequence, ship owners have been seeking solutions to comply with new emission limits and Liquefied natural gas (LNG) currently represents an economic alternative energy source with a reduced environmental impact. The growing interest for LNG fueled vessels is linked to the development of a small-scale LNG sites network as part of the supply chain, as well as an increase in road transportation of LNG.

Despite the positive safety record of LNG transportation industry, the fire and explosion hazards posed by this substance cannot be disregarded. Storage areas are identified as one of the most vulnerable part of a process plant and fire scenarios represent a frequent cause of accident escalation (Casal and Darbra, 2013). As highlighted by Iannaccone et al. (2019), the potential damage extent resulting from accident escalation involving LNG storage tanks is the largest among all the other process units of a typical small-scale LNG site. Moreover, fire exposure of pressurized cryogenic storage tankers has resulted in critical events, such as boiling liquid expanding vapor explosion, fireballs and missiles projection (Planas et al., 2015). It is therefore important that hazards related to accidental fire exposure are taken into account in the design, operation and management of installation devoted to LNG transportation and storage. The present work focuses on analysis of the response of double-walled LNG tanks exposed to thermal radiation from distant hydrocarbon pool fire. A 2D CFD approach was chosen for the analysis. This kind of approach was proved to be more effective than the use of traditional lumped models, which suffer several limitations and are not able to predict pressurization and temperature distributions with confidence (Scarponi et al., 2018a).

Paper Received: 12 January 2020; Revised: 1 May 2020; Accepted: 20 August 2020
Please cite this article as: Iannaccone T., Scarponi G.E., Landucci G., Cozzani V., 2020, Lng Tanks Exposed to Distant Pool Fires: a CFD Study, Chemical Engineering Transactions, 82, 373-378 DOI:10.3303/CET2082063

2. Model description

2.1 Numerical setup

The problem under analysis is transient, turbulent (values of Rayleigh number higher than 10^9 were found in a preliminary dimensional analysis), and multiphase in nature.
Following the approach proposed by Scarponi et al. (2019) in a similar work on LPG tanks, the k-ω SST turbulence model (without the use of wall functions) was selected to account for turbulence effects. The volume of fluid model was selected as multiphase model, since it is suitable for simulating the behavior of two immiscible phases (Liquid and Vapor in this case), tracking the interface between them (Hirt and Nichols, 1981). To calculate mass transfer rates from liquid to vapor phases and vice-versa (indicated by terms $m_{L\to V}$ and $m_{V\to L}$ in Eq. (1) and Eq. (2), respectively), the evaporation-condensation model implemented in ANSYS Fluent (Lee, 1979) was used, considering default evaporation/condensation frequency values (C_{Evap} and C_{Cond}) as suggested in a similar work (D'Aulisa et al., 2014). For each cell on the domain, the model determines whether evaporation or condensation take place based on the cell temperature (T): if T is above the saturation temperature (T_{sat}) calculated at the cell pressure, part of the liquid phase will evaporate, otherwise condensation will occur:

$$m_{L\to V} = C_{Evap}\alpha_L\rho_L\left(\frac{T-T_{sat}}{T_{sat}}\right) \quad (1)$$

$$m_{V\to L} = C_{Cond}\alpha_V\rho_V\left(\frac{T_{sat}-T}{T_{sat}}\right) \quad (2)$$

The terms α and ρ in Eq. (1) and Eq. (2) indicate respectively the volume fraction and density of liquid (L) and vapor (V) phases.
To avoid the introduction of uncertainties related to material composition, LNG was modelled as pure methane. Peng –Robinson equation of state was used to model vapor phase density, whilst liquid properties were expressed as a function of temperature based on data from Lemmon et al. (2020). Thermal properties of the insulating material were collected from Beikircher and Demharter (2013). The duration of all simulations carried out was set equal to two hours.
To model the time evolution of the systems, a first-order implicit scheme with a fixed time step of 0.01 s was used. Spatial discretization of density, momentum, energy and turbulence model equations was performed with a second order upwind scheme. Pressure equation was discretized using the PRESTO! scheme, while volume fraction equations were solved with the Geo-Reconstruction scheme. Pressure-velocity coupling was achieved by using the SIMPLEC (Semi-Implicit Method for Pressure Linked Equations-Consistent) algorithm. The key governing equations of the 2D CFD model are reported in Scarponi et al. (2018a).

2.2 Case studies

Two different double-walled pressurized cryogenic tanks types were analyzed. Each one was simulated considering three different filling degrees. In this type of tanks, the annular space between tank inner and outer walls is filled with a thermal insulating material, which is typically kept under vacuum conditions to enhance insulating performance.
The first case study (referred to as Case A in the following) is based on a typical tank size for naval applications, while the other case (referred to as Case B) is representative of a standard trailer tank used for road transportation of LNG. Tank construction details of the case studies are reported in Table 1, along with initial conditions considered.
For both cases A and B it was assumed that the tank insulation material is made of perlite grains. Past accidents and fire tests have shown that fire exposure is likely to induce loss of vacuum in the annular gap due to thermal deformation of the outer tank wall (Hulsbosch-dam et al., 2017), thus reducing the insulation effectiveness. Therefore, to analyze a worst-case scenario condition, vacuum was considered to be lost since the beginning of the simulation. A constant thermal conductivity value of 0.3 W/(m K) was considered for the damaged perlite insulation, based on the outcomes of the study carried out by Beikircher and Demharter (2013).

2.3 Calculation grid and initial conditions

The CFD simulations were carried out using the software ANSYS® Fluent® 18.2.0 and considered, as computational domain, a 2D vertical (and perpendicular to the axial direction) section of the cylindrical tank (see Figure 1a). Two unstructured meshes (one for each case study analyzed) were generated using ANSYS® Meshing™, the meshing parameters are reported in Table 2. The grid was refined in the proximity of the inner wall in order to accurately resolve the temperature and velocity profile in this region, as required by k-ω SST turbulence model. Such refinement was achieved through the creation of inflation layers.

For both case studies, the tank lading was assumed to be at saturation condition according to the values of temperature and pressure reported in Table 1, with uniform temperature throughout the fluid domain (both liquid and vapor). The fluid inside the tank was initially at rest and turbulent kinetic energy and specific dissipation rate were initialized at 10^{-9} m^2/s^2 and 10^{-3} s^{-1} respectively.

Table 1: Construction details and initial conditions considered for the case studies.

Case ID	Filling degree [%]	Initial pressure [bar]	Initial temperature [K]	Inner diameter [m]	Insulation thickness [m]	Length [m]	MAWP* [bar]	Nominal capacity [m^3]
Marine LNG storage tank								
A85	85	6.0	138.73	4.3	0.25	16.5	11.0	240
A50	50							
A15	15							
Road trailer LNG tank								
B85	85	1.0	111.66	2.3	0.12	13.8	3.0	58.0
B50	50							
B15	15							

* MAWP: Maximum Allowed Working Pressure, assumed equal to tank design pressure.

A linear temperature gradient was imposed for perlite insulation: the temperature decreases linearly (along the wall radius) from T_{amb} (considered equal to 16 °C) and the initial saturation temperature of methane, as reported in Table 1.

Table 2: Details of mesh features.

Case ID	Mesh elements	First layer thickness [m]	Inflation layers	Maximum cell size [m]
A85	58,914	7.0×10^{-4}	40	0.030
A50				
A15				
B85	137,064	7.0×10^{-5}	50	0.010
B50				
B15				

2.4 Fire characterization and boundary condition

An LNG pool fire was taken as reference scenario for the present study. This may result following a release occurring during fuel transfer operations. The amount of LNG spilled from a 3" (76.2 mm) diameter transfer hose was used as input for the estimation of pool diameter and flame geometry using well-established consequence models (Van Den Bosh and Weterings, 2005). The pool fire was modelled following a solid flame approach. To account for the effect of the wind on the flame shape, this was modelled as a tilted cylinder. The pool fire considered in both case studies has a diameter of 3.2 m, a flame height of 11.9 m and is assumed to be distant 15 m from the tank center. The flame is tilted by an angle of 57° due to the considered wind velocity of 5 m/s.

The incident radiation induced by the pool fire over the tank wall is not uniform. Thus, a preliminary analysis was required to set the appropriate boundary condition, representative of the fire scenario under analysis. This was done by following the approach proposed by Scarponi et al. (2018b), who studied the exposure of LPG tanks to a distant fire front. Neglecting the fraction of radiation absorbed by the atmosphere and assuming the fire as an emitting surface with a constant equivalent black body temperature ($T_{f,BB}$, that was set to a value of 860 °C), the incident radiation (I_P) at point P on the tank surface can be expressed as follows:

$$I_P = \sigma \times (f_{P\to f} \times T_{f,BB}^4 + (1 - f_{P\to f}) \times T_{amb}^4) \quad (3)$$

where σ is the Stefan-Boltzmann constant and T_{amb} is the ambient temperature (set to 16 °C). The term $f_{P\to f}$ is the view factor between point P and the fire. With reference to Figure 1a, the analytical expression of the view factor between a tank element T_i with area dA_1 and an element F_j on the surface of the pool fire, with area dA_2 is:

$$F_{T_i F_j} = \frac{1}{A_1}\int_{A2}\int_{A1} \frac{\cos\alpha_1 \cos\alpha_2}{\pi S^2} dA_1 dA_2 \quad (4)$$

where α_1 and α_2 indicate the angle between the segment S (connecting T_i and F_j) and surface normal vectors n_1 and n_2 respectively.

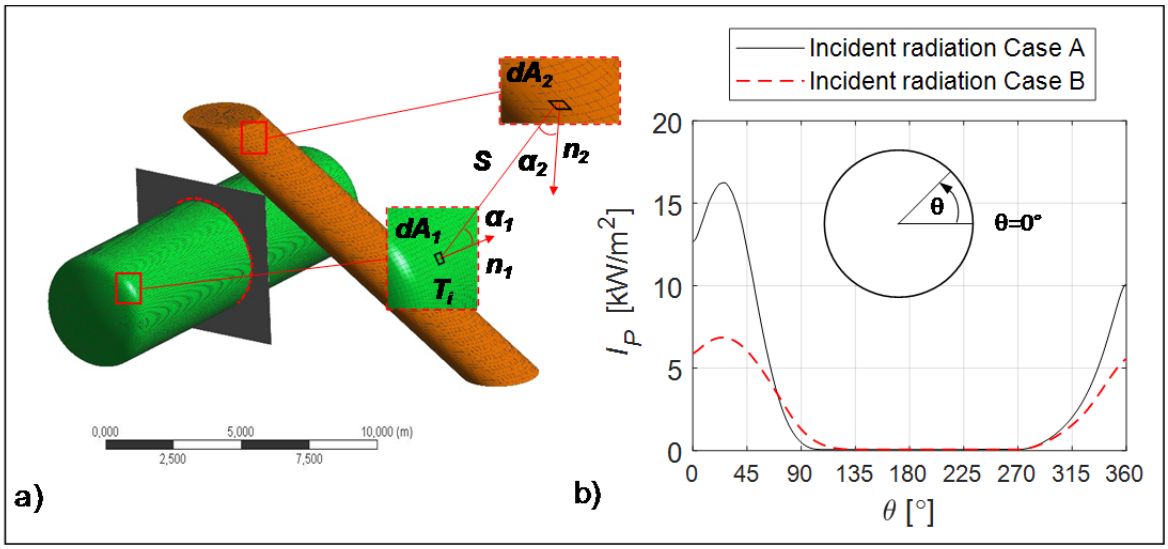

Figure 1: Meshed 3D geometries of pool fire and tank used for view factor calculation (a). Panel (b) shows the variation of the incident radiation as a function of the angular coordinate on the central circular section.

The tank outer wall and the surface of the fire were discretized using grid elements with a maximum edge size of 0.1 and 0.2 m, respectively. Eq. (4) was solved numerically using a MATLAB® script, approximating the integral with a summation over all mesh elements of the fire. In this way, view factors were calculated for each mesh element on the tank surface. Thus, using Eq. (3), it was possible to obtain the values of the incident radiation over the red dashed line reported in Figure 1a, representing the external boundary of the 2D computational domain considered for the CFD simulations. The result of this calculation for the two tanks under analysis are reported in Figure 1b.
At this point, Eq. (5) can be used to calculate an equivalent black body temperature, $T_{BB,eq}$, representative of the incident radiation hitting the tank wall, that will be used for the definition of the boundary condition.

$$T^4_{BB,eq.} = \frac{I_P}{\sigma} \quad (5)$$

Knowing $T_{BB,eq}$, the solver calculates the entering heat flux ($\dot{q}''_P$) for each point *P* on the outer wall of the tank using according to Eq. (6).

$$\dot{q}''_P = \sigma \times \varepsilon_{wall} \times (T^4_{BB,eq.} - T^4_{wall}) \quad (6)$$

Where, ε_{wall} is the tank outer wall emissivity (assumed equal to 0.7), $T_{BB,eq}$ is the pool fire equivalent black body temperature and T_{wall} is the tank outer wall temperature.

3. Results and discussion

Due to the novelty of LNG fueled transportation technologies, there are currently no available experimental data concerning heat effects on storage tanks caused by distant fires that can be used to validate the model. Only a set of experimental bonfire tests challenged the possibility of a catastrophic rupture of cryogenic vessels engulfed by flames (Kamperveen et al., 2016). The heat load induced by external fires on storage tanks determines a temperature increase of the tank lading, promoting evaporation of the liquid phase and, consequently tank pressurization. This is clearly visible in Figure 2, reporting the dynamic evolution of tank pressure for the six case studies. It can be observed that the pressurization rate increases with the decrease of the filling degree. This result is in accordance with heat leaks experimental tests carried out with liquid

hydrogen (Van Drew et al., 1992). For both the tanks analyzed the pressure increase is limited to 1 bar above the initial pressure value.
Comparing Figure 2a and 2b, it can be noticed how different operative conditions and tank size affect the pressure build-up: while cases A show a significant time lag (about 45 minutes) before the pressure starts to rise, pressurization for case study B is not delayed.

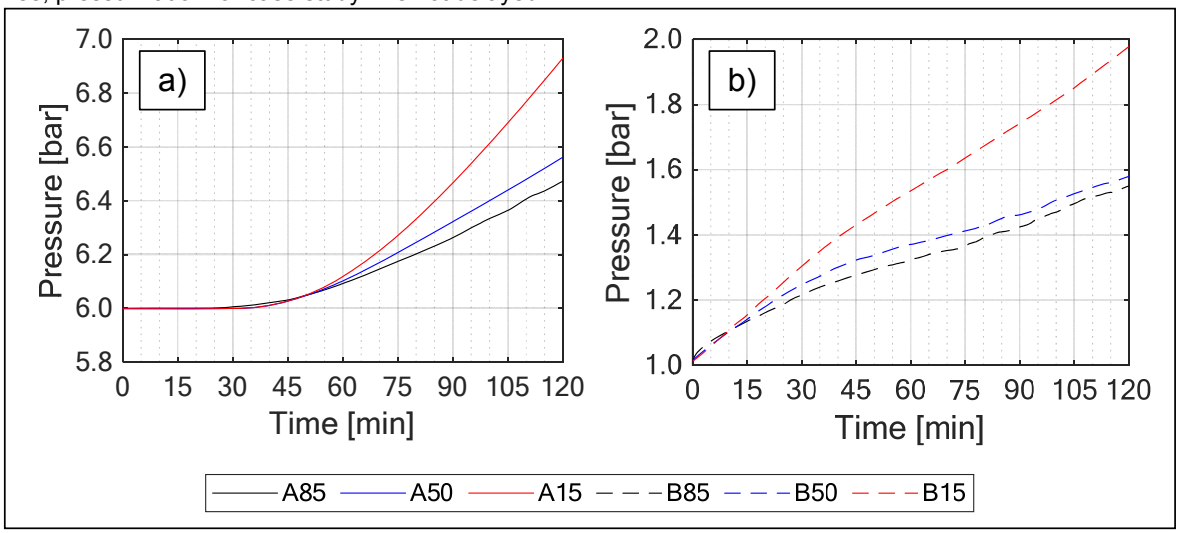

Figure 2: Pressurization curves obtained for the case studies listed in Table 1.

In summary, for all the cases, the pressure reached inside the tank after two hours of pool fire exposure remains always below the MAWP values reported in Table 1, suggesting that tank integrity is not threatened by this kind of fire scenario.
However, pressure is not the only factor having the potential to induce tank rupture. Degradation of steel structural properties due to high temperatures and local thermal stresses may also result in tank failures. Figure 3 compares the variation of tank's inner wall temperatures with position for the case studies at different times. It is clear how the higher heat transfer coefficients for the liquid phase contribute to keep the wetted part of tank wall at lower temperatures than the wall portion in contact with the vapor, possibly inducing thermal stresses. Moreover, the temperature predicted for cases B is far greater than the correspondent cases A. This effect could be linked to the thinner insulation layer of Case B that increases the heat flux reaching the inner wall and to a higher surface-to-volume ratio characteristic of smaller diameter tank. However, in all the six cases, the maximum temperature reached by the wall section in contact with the vapor region is always lower than 323 K, which is the maximum design temperature for static vacuum insulated austenitic steel vessels as specified in the European standard EN 13458-2:2002 (European committee for standardization, 2002).

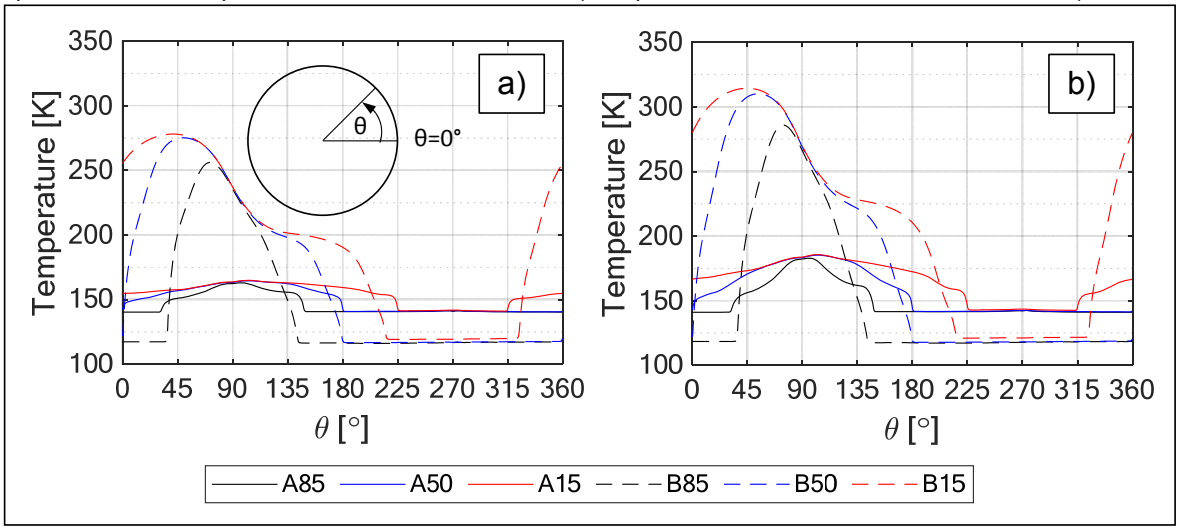

Figure 3: Inner wall temperature profiles at 90 min (a) and 120 min (b) as a function of radial position θ.

4. Conclusions

The CFD modelling approach presented in this work allowed to study the response of LNG tanks to a complex scenario such as a distant pool fire and to analyze the influence of the tank size and filling degree on vessel pressure build-up and wall temperature rise. It was observed that the pressurization rate increases with lower tank filling degrees, independently from tank size and initial conditions. It was found that road trailer tanks (Case B) start to pressurize as soon as they are exposed to the fire conditions, whereas marine LNG storage tanks (Case A) remain almost unaffected by the investigated pool fire scenario up to about 45 minutes. The analysis of tank inner wall temperatures shows that greater temperature differences between liquid and vapor regions of the vessel can be expected for larger tanks (Case B). This situation may generate localized thermal stresses in proximity of vapor-liquid interface that could weaken the tank structure and induce local yielding. A more detailed analysis of tank structural integrity with finite elements software would be required to further investigate this aspect. Results produced in this work could support the setup for such analysis.

In summary, values of pressure and wall temperature obtained in the CFD simulation suggest that the impact of distant pool fires resulting from moderate LNG leakages will not be critical for pressurized cryogenic tanks even if their insulation is compromised. However, this does not exclude that more severe fires (e.g. full engulfment fires) might represent a threat for tank integrity, especially for the smaller ones, possibly leading to accident escalation.

The results of this work can provide a basis for a broader accidental scenario modelling covering different fire and operative conditions. Pressurization dynamics, walls and tank lading temperature data can also represent a valuable source of information for emergency responders, providing useful information to evaluate possible tank failure conditions.

References

Beikircher, T., Demharter, M., 2013, Heat Transport in Evacuated Perlite Powders for Super-Insulated Long-Term Storages up to 300 °C, J. Heat Transfer, 135, 051301-1-051301-11.

Casal, J., Darbra, R.-M., 2013, Analysis of Past Accidents and Relevant Case-Histories, Domino Eff. Process Ind., 12–29.

D'Aulisa, A., Tugnoli, A., Cozzani, V., Landucci, G., Birk, A.M., 2014, CFD modeling of LPG vessels under fire exposure conditions, AIChE J., 60, 4292–4305.

European committee for standardization, 2002, Cryogenic vessels - Static vacuum insulated vessels - Part 2: Design, fabrication, inspection and testing, CEN, Brussels, Belgium.

Hirt, C., Nichols, B., 1981, Volume of fluid (VOF) method for the dynamics of free boundaries, J. Comput. Phys., 39, 201–225.

Hulsbosch-dam, C., Atli-veltin, B., Kamperveen, J., Velthuis, H., Reinders, J., Spruijt, M., 2017, Thermodynamic aspects of an LNG tank in fire and experimental validation, EPJ Web Conf., 143, 0–5.

Iannaccone, T., Ovidi, F., Scarponi, G.E., Landucci, G., Cozzani, V., 2019, Safety of Cryogenic Storage Facilities of Flammable Gases, Chem. Eng. Trans., 77, 535-540.

Kamperveen, J., Spruijt, M., Reinders, J., 2016, Heat load resistance of cryogenic storage tanks – Results of LNG Safety Program, Utrecht, The Netherlands.

Lee, W.H., 1979, A pressure iteration scheme for two-phase modeling, Los Alamos Sci. Lab., Los Alamos, NM, USA.

Lemmon, E.W., McLinden, M.O., Friend, D.G., 2020, Thermophysical Properties of Fluid Systems, Chapter in: Linstrom, P.J., Mallard, W.G. (Eds.), NIST Chemistry WebBook, NIST Standard Reference Database Number 69. National Institute of Standards and Technology, Gaithersburg MD, USA.

Planas, E., Pastor, E., Casal, J., Bonilla, J.M., 2015, Analysis of the boiling liquid expanding vapor explosion (BLEVE) of a liquefied natural gas road tanker: The Zarzalico accident, J. Loss Prev. Process Ind., 34, 127–138.

Scarponi, G.E., Landucci, G., Birk, A.M., Cozzani, V., 2019, An innovative three-dimensional approach for the simulation of pressure vessels exposed to fire, J. Loss Prev. Process Ind., 61, 160–173.

Scarponi, G.E., Landucci, G., Birk, A.M., Cozzani, V., 2018a, LPG vessels exposed to fire: Scale effects on pressure build-up, J. Loss Prev. Process Ind., 56, 342-358.

Scarponi, G.E., Landucci, G., Heymes, F., Cozzani, V., 2018b, Experimental and numerical study of the behavior of LPG tanks exposed to wildland fires, Process Saf. Environ. Prot., 114, 251–270.

Van Den Bosh C.J.H., Weterings R.A.P., 2005, Methods for the Calculation of Physical Effects (Yellow Book), Committee for the Prevention of Disasters, The Hague, The Netherlands.

Van Drew, N.T., Lin, C.S., Hasan, M.M., 1992, Self-Pressurization of a Flightweight Liquid Hydrogen Tank: Effects of Fill Level at Low Wall Heat Flux, NASA Lewis Research Center, Cleveland, OH, USA.